Effect of Air Blowing on the Morphology and Nanofiber Properties of Blowing-Assisted Electrospun Polycarbonates

Hung-Yi Hsiao,[1] Chao-Ming Huang,[2] Yi-Yu Liu,[1] Yu-Cheng Kuo,[1] Hui Chen[1]

[1]*Department of Chemical and Materials Engineering, National Central University, Jhongli, Taiwan*
[2]*Department of Materials Engineering, Kun Shan University, Tainan, Taiwan*

Received 25 August 2010; accepted 5 September 2011
DOI 10.1002/app.35599
Published online 7 December 2011 in Wiley Online Library (wileyonlinelibrary.com).

ABSTRACT: Polycarbonate (PC) nanofibers are prepared using the air blowing-assisted electrospinning process. The effects of air blowing pressure and PC solution concentration on the physical properties of fibers and the filtration performance of the nanofiber web are investigated. The air blowing-assisted electrospinning process produces fewer beads and smaller nanofiber diameters compared with those obtained without air blowing. Uniform PC nanofibers with an average fiber diameter of about 0.170 μm are obtained using an applied voltage of 40 kV, an air blowing pressure of 0.3 MPa, a PC solution concentration of 16%, and a tip-to-collection-screen distance (TCD) of 25 cm. The filtration efficiency improvement of the air blowing-assisted electrospun web can be attributed to the narrow distribution of fiber diameter and small mean flow pore size of the electrospun web. Performance results show that the air blowing-assisted electrospinning process can be applied to produce PC nanofiber mats with high-quality filtration. © 2011 Wiley Periodicals, Inc. J Appl Polym Sci 124: 4904–4914, 2012

Key words: polycarbonates; morphology; nanofibers; blowing-assisted multi-jet electrospinning; nanofiber mats

INTRODUCTION

Nanofibers have attracted interest in many fields due to their large specific surface area, high aspect ratio, and high porosity with a small pore size as a result of random web deposition.[1] At present, nanofibers can be prepared by splitting bicomponent fibers[2] or using the self-assembly method,[3] template synthesis,[4] or electrospinning.[5] Electrospinning is considered the most efficient and versatile technique for generating ultra-thin fibers with diameters on the nano to micro scale.[6] More than 100 polymers have been electrospun into ultra-fine fibers.[1,7] However, few studies have been conducted on polycarbonate (PC) nanofibers.

PC is a thermoplastic material that is widely used as an injection molding material due to its excellent physical and mechanical properties such as heat resistance and high impact strength.[8,9] Many researchers have investigated the formation of PC nanofibers, but few have used electrospinning. Recently, several studies have used electrospinning to fabricate micro- to nanoporous PC membranes and investigated the effect of the solvent and process parameters on the morphology of the membranes electrospun from the PC solution.[10–12] Kim et al.[8] prepared antimicrobial nanofibers by electrospinning PC solution with benzyl triethylammoniumchloride. Moon et al.[13] developed a method for preparing electrospun PC nanofibers. PC electrospun webs with excellent biocompatibility and porosity have potential application as filters,[8] scaffolds for tissue engineering,[14] and composites.[15] Although nanofibers have been generated by electrospinning, most studies have focused on the structure and morphology of the nanofibers; few studies have reported the properties of electrospun webs. Electrospinning, which is an effective and versatile approach for generating polymeric nanofibers using a high-voltage electrostatic field, has recently received a lot of attention for the production of filter media for high-filtration-efficiency air filters.[16–18] In a typical process, an electrostatic potential is applied between droplets of a polymer solution, or melt, which are passed through a capillary needle, and a grounded collection target. When the applied electrostatic forces overcome the surface tension of the droplets, a charged fluid of polymer solution is ejected as a jet of a Taylor cone.[19] The electrostatic forces draw the polymer jet thousands of times, making it very thin. Finally, the solvent evaporates and the deposited nanofibers are collected on the grounded target as nonwoven mats.[20] In principle, the stretching of the polymer jet is governed by the electrostatic force and the rheology of the solution.[21] In general, the electrospinning process has two distinct stages. In the first stage, a polymer jet is accelerated by the

Correspondence to: H. Chen (huichen@cc.ncu.edu.tw).

electrostatic force, ejected from the tube, and then thinned until the instability point. Models for electrospun jets in this stage have been proposed by Feng,[21,22] Hohman,[23] and Reneker et al.[24] In the second stage, the polymer jet becomes unstable and becomes either a beaded jet or a chaotic jet. Carroll et al.[25] conducted theoretical and experimental investigations of the axisymmetric instability. Theoretical models for viscoelastic jets have been proposed by Feng,[21] Caroll,[25] and Reneker et al.[26] In addition, Yu et al.[27] investigated the effect of elasticity on the formation of beaded electrospun fibers. A lot of researchers have demonstrated the important role of extensional rheology in electrospinning. However, no detailed investigation has been conducted on the influence of the rheological properties of PC solution on the electrospinning process. Therefore, the present study investigates the relationship between the rheology of PC solution and the morphology of PC fibers. Electrospinning usually has relatively low yields compared with those of traditional spinning processes.[28] Many studies have indicated that high throughput can be achieved using multiple-jet spinnerets.[29–31] Recently, some researchers have prepared polymer nanofibers using blowing-assisted electrospinning, which combines the process of electrospinning with air blowing around the spinneret. Wang et al.[32] and Um et al.[33] demonstrated the preparation of hyaluronic acid nanofibers using blowing-assisted electrospinning. Peng et al.[34] combined electroblowing and the sol–gel reaction to generate mesoporous silica fibers. Kong et al.[28] investigated the effect of applied voltage and air blowing pressure on nanofiber mat deposition by the electroblowing of polyvinyl alcohol. Lin et al.[35] and Wang et al.[36] combined electrospinning with a gas-jet device to prepare poly(ether sulfone) and poly(ester imide) nanofibers. However, there has been few research on the blowing-assisted electrospinning of PC.

In this article, the multiple-jet blowing-assisted electrospinning process is used to prepare PC nanofibers. The process parameters include air blowing pressure, PC solution concentration, and the feed rate of the solution. The filtration characteristics such as the Frazier air permeability, filtration efficiency, and pressure drop of the air blowing-assisted electrospun PC web are evaluated. The filtration performance for various mean flow pore diameters of the electrospun web is measured.

EXPERIMENTAL SECTION

Materials

PC (Mw 43,000) of bisphenol A with a melt index of 7 g/10 min (300°C/1.2 kg) was purchased from Sigma-Aldrich. Tetrahydrofuran (THF) was purchased from Mallinckrodt Baker, and *N*,*N*-dimethylacetamide (DMAc) was purchased from Tedia. PC solutions for electrospinning with concentrations of 12, 14, and 16% (w/v) were prepared by dissolving the polymer in a mixture of DMAc/THF (1 : 1, v/v) under magnetic stirring at 60°C for 12 h.

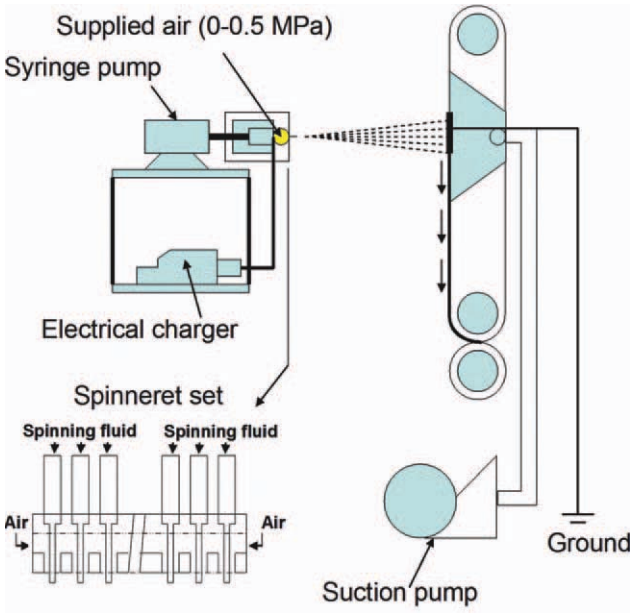

Figure 1 Blowing-assisted multiple-jet electrospinning setup. [Color figure can be viewed in the online issue, which is available at wileyonlinelibrary.com.]

A schematic diagram of the air blowing-assisted multiple-jet electrospinning apparatus is shown in Figure 1. The setup includes a 16-needle assembly in a spinneret pack that was modified to have air blowing around the needles. The PC solution, held in four sets of 25-mL syringes connected to a four-tube distributor, was delivered into a 23-G injection needle of the spinneret pack through Teflon tubing by a syringe pump (KDS-200, KD Scientific, USA). The feed rate of the polymer solution ranged from 0.75 to 3.0 mL/h. A positive high-voltage power supply (SIMCO, Industrial Static Control, USA) was used to charge the spinning dope of PC solution by directly fastening the electrode to the metal needle spinneret pack. The weight per square meter of the polypropylene (PP) nonwoven support (Mytrex Industries, Taiwan) was 15 g/m^2. The PP nonwoven support was placed on a stainless steel collecting screen, which was grounded to collect the electrospun webs. The electric field was set to 40 kV and the distance between the two electrodes was 25 cm. For the blowing-assisted electrospinning process, an air compressor was attached to the electrospinning apparatus to simultaneously provide electrical force and air blowing driving force to fabricate the nanofibers from the polymer solution.

TABLE I
Filtration Efficiency and Pressure Drop of PP Nonwoven Web for Various Face Velocities

	Face velocity (cm/s)				
	2.67	5.33	8.0	10.67	13.33
Filtration efficiency (%)	71.9	64.5	60.1	55.5	51.8
Pressure drop (mmH_2O)	1.0	2.0	3.2	4.3	5.4

Solution characterizations

The viscosities of PC in DMAc/THF solutions were measured in a Brookfield digital viscometer (Model RVT) at 25°C. Surface tension measurements were measured using a tensiometer (CBVP-A3) at 25°C. The electrical conductivity of the PC solutions was measured using a conductivity meter (WTW, Cond 315i) at 25°C. The rheological properties of the PC solutions were determined using a rheometer (ARES-LS1, TI Instruments). A 50-mm-thick plate and a 0.6-mm gap were used. Dynamic strain sweeps (at constant frequencies of 0.1, 0.5, 1, and 10 rad/s, with the strain amplitude varied from 0.03 to 100%) were conducted to identify the region of linear viscoelasticity. Dynamic frequency sweeps (at a constant linear strain and frequencies ranging from 0.1 to 100 rad/s at 25°C) were performed to determine the linear viscoelastic properties of the storage modulus (G′) and loss modulus (G″).

Scanning electron microscope characterization

The fiber morphology was observed using a scanning electron microscope (SEM; JSM-6480 LV, JEOL) with an acceleration voltage of 5 kV. Before SEM observation, all of the samples cut from the electrospun webs were sputter-coated with gold using an EMITECH K550 sputter coater for analysis. The average fiber diameters of the air blowing-assisted multiple-jet electrospun nanofibers were determined by SEM micrographs from a population of more than 200 fibers using ImageJ software, which was developed by Upper Austria University of Applied Sciences.[37]

Measurement of bead density

Bead density was measured from SEM micrographs. The beads were counted and the area of each bead was measured using ImageJ software. The bead density was then calculated using:[38]

$$\text{Bead density} = (\text{Area of beads in image}/\text{Area of image}) \times 100$$

Frazier air permeability and mean flow pore size

The nanofiber mat/PP nonwoven web was cut into 5.5-cm-diameter disks and coated with Gatwick wetting agent for analysis. The Frazier air permeability and mean flow pore size were determined using a capillary flow porometer (1200AEX, American PMI). The wet up/dry down mode of operation was used. The Gatwick wetting liquid was allowed to fill the pores in the mat and nonreacting air was allowed to displace the liquid from the pores. The air pressure and flow rates through wet and dry samples were accurately measured. The air pressure required to flush out the liquid from the pores and to pass through the mat is given by:

$$D = 4\gamma \cos\theta / p,$$

where D is the pore diameter, γ is the surface tension of the Gatwick liquid, θ is the contact angle of the Gatwick liquid, and p is the differential air pressure. From the measured air pressure and flow rates, the Frazier air permeability at a pressure of 12.7 mm H_2O and the mean flow pore size were calculated. The mean flow pore size and Frazier air permeability of the PP nonwoven web were about 9.8 μm and 1.35 $m^3/m^2/min$, respectively.

Filtration efficiency

The filtration performance, namely the filtration efficiency and pressure drop, of the air blowing-assisted electrospun web deposited on the PP nonwoven support was evaluated. The filtration efficiency and pressure drop were determined using an aerosol of 0.3 μm NaCl particles at face velocities in the range of 2.67–13.33 cm/s on a TSI Model 8130 filtration tester. The results of filtration efficiency and pressure drop of the PP nonwoven web are listed in Table I.

RESULTS AND DISCUSSION

Solution properties

Table II shows the viscosity, surface tension, and conductivity of the PC solutions. In experiments, the surface tension and conductivity did not obviously change when the solution concentration of PC in DMAc/THF was increased from 12 to 16%, whereas the viscosity increased from 54 to 128 mPa s. Figure 2 shows the linear viscoelastic properties of the storage

TABLE II
Viscosity, Surface Tension, and Conductivity of PC Solutions

Sample (%)	Viscosity (mPa s)	Surface tension (mN/m)	Conductivity (μS/cm)
12 PC	54	30.6	0.6
14 PC	81	30.6	0.7
16 PC	128	30.8	0.7

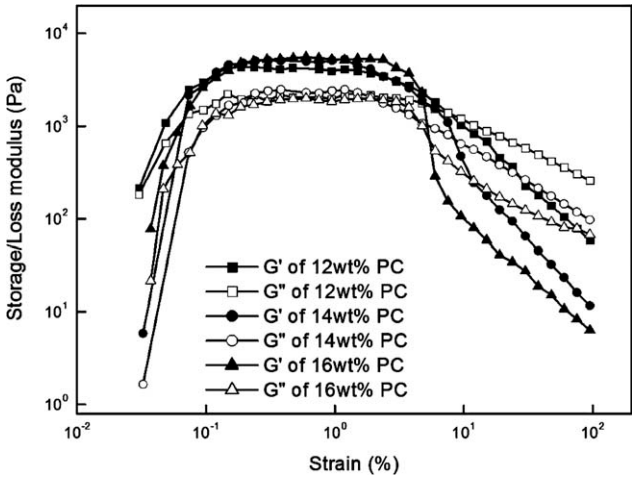

Figure 2 Dynamic strain sweeps of PC solutions at a constant frequency of 0.5 rad/s for (a) 12%, (b) 14%, and (c) 16% PC solutions.

modulus (G′) and loss modulus (G″) vs. strain. G′ and G″ did not change with the strain in the range of 0.15–1.88% at a constant frequency of 0.5 rad/s. Therefore, the dynamic viscoelastic properties of the PC solution were investigated at a strain amplitude of 1%. Figure 3 shows a comparison of G′ and G″ for 12, 14, and 16% PC solutions. For the 12% PC solution, G″ is higher than G′ over the entire frequency range, showing that this PC solution is viscous. For 14 and 16% PC solutions, G′ is higher than G″ over the entire frequency range, indicating that these PC solutions are elastic. When the PC solution concentration was increased from 12 to 16%, the viscoelasticity of the PC solution increased.

Fiber morphology

Polymer concentration and viscoelastic properties of the PC solutions are considered significant parameters in the electrospinning process.[26,39,40] It was found that the morphology of the PC electrospun nanofibers greatly depends on the viscoelastic properties of the PC solution as shown in Figures 3 and 4. The 12% PC solution was viscous, therefore larger droplets and beads were obtained [Fig. 4(a)]. In this case, the lack of elasticity of the PC solution prohibits the formation of uniform fibers, resulting in the formation of droplets or bead-on-string structures. When the PC solution concentration was increased from 12 to 16%, the PC solution became more elastic and thus more fibers were obtained and the number of beads decreased [Fig. 4(b,c)]. The relationship between the rheology of the PC solution and the morphology of the PC fibers is consistent with the results reported in the published reports.[27,41,42] The effect of polymer concentration on the morphology of air blowing-assisted electrospun nanofibers was investigated. The other parameters of the electrospinning process were set as follows: the applied voltage was 40 kV, the TCD was 25 cm, the multiple-jet spinneret had 16 metal 23G syringe needles, and the feed flow rate of the polymeric solution was 2.25 mL/h. Figure 4 shows SEM images and diameter distributions of PC electrospun nanofibers obtained using PC concentrations of 12, 14, and 16% in DMAc/THF. It was found that the morphology of the obtained PC fibers significantly changed with PC concentration. Large droplets and beads that accumulated to form a film-like structure were observed for the 12% PC solution samples as shown in Fig. 4(a). For the 14% PC solution [Fig. 4(b)], more beads with fibers were obtained. For the 16% PC solution [Fig. 4(c)], the electrospun nanofibers had fewer beads but more fibers than those obtained for 12 and 14% PC solution samples. The number of nanofibers increased with increasing polymer solution concentration; however, nanofibers with few beads were not obtained due to the limited change in the evaporation rate of the solvent.

Wang et al.[32] found that air blowing could be used to improve the formation of electrospun nanofibers. To investigate the effect of air pressure on morphology, the parameters were fixed as follows: the applied voltage was 40 kV and the feed flow rate of the polymeric solution was 2.25 mL/h. Figure 5 shows SEM images and diameter distributions of electrospun nanofibers obtained from 12% PC solution with the assistance of air blowing with air pressures in the range of 0.1–0.5 MPa. The shape of beads gradually changed from spherical to fiber-like [Fig. 5(a)]. When the air blowing pressure was above 0.3 MPa [Fig. 5(b)], more fibers than beads were formed. Figures 6 and 7 show SEM images and diameter distributions of electrospun nanofibers with

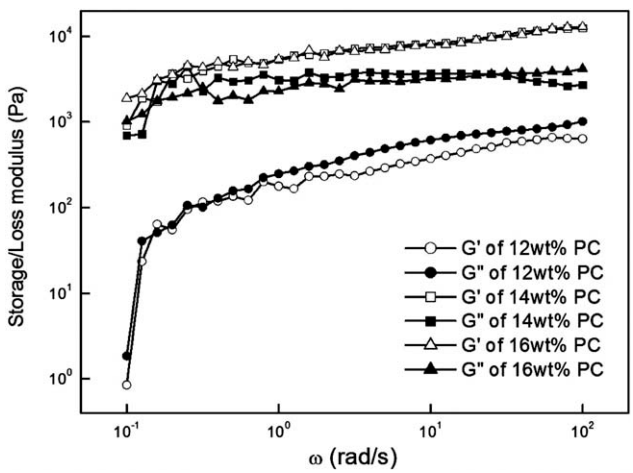

Figure 3 Storage modulus (G′) and loss modulus (G″) as functions of frequency (ω) for (a) 12%, (b) 14%, and (c) 16% PC solutions.

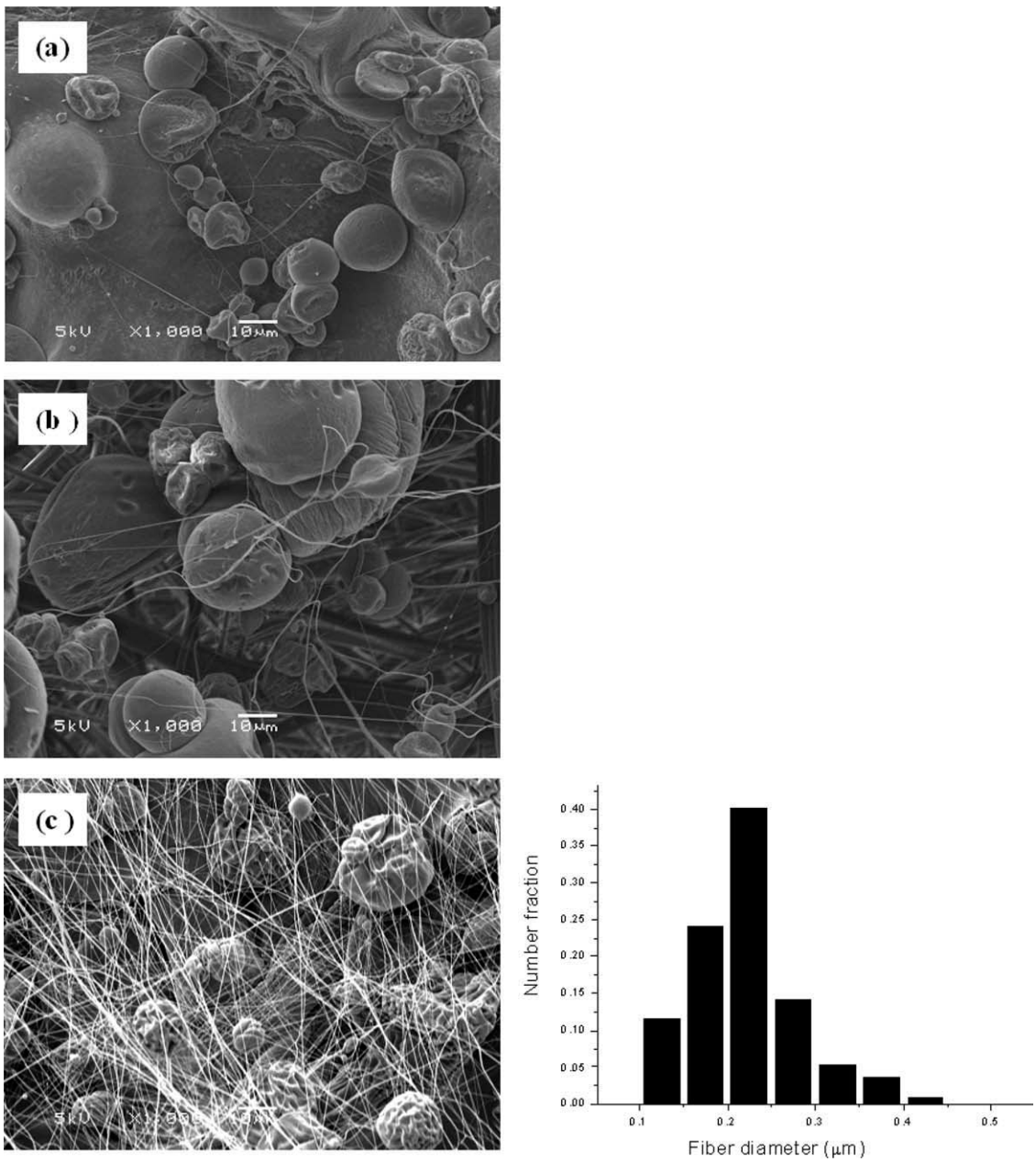

Figure 4 SEM images of fiber formations obtained using (a) 12%, (b) 14%, and (c) 16% PC solutions (with diameter distribution on the right).

air blowing-assisted electrospinning conducted with 14 and 16% PC solutions, respectively. It can be seen that air blowing pressure has a big effect on bead formation. The bead size decreases with increasing air blowing pressure. To further investigate the change of bead formation, the bead density was calculated. Figure 8 shows the effect of air blowing pressure on the bead density of various samples. When the air blowing pressure was increased from 0.0 to 0.5 MPa, the bead density decreased from 80.54 to 11.1%, 46.45 to 5.33%, and 21.0 to 6.04% for 12, 14, and 16% PC solutions, respectively. The bead density of the nanofibers decreases with increasing air blowing pressure, because air blowing increases the driving force, which ultimately may enhance the stretching imposed upon the forming fibers and thus fewer beaded fibers.[32]

Fiber diameter

The gas flow rate and polymer solution concentration during gas-jet/electrospinning are the most important factors in the electrospinning process.[35,36] Figure 9 shows the average diameter of electrospun PC nanofibers generated at various air blowing pressures and polymer solution concentrations. When

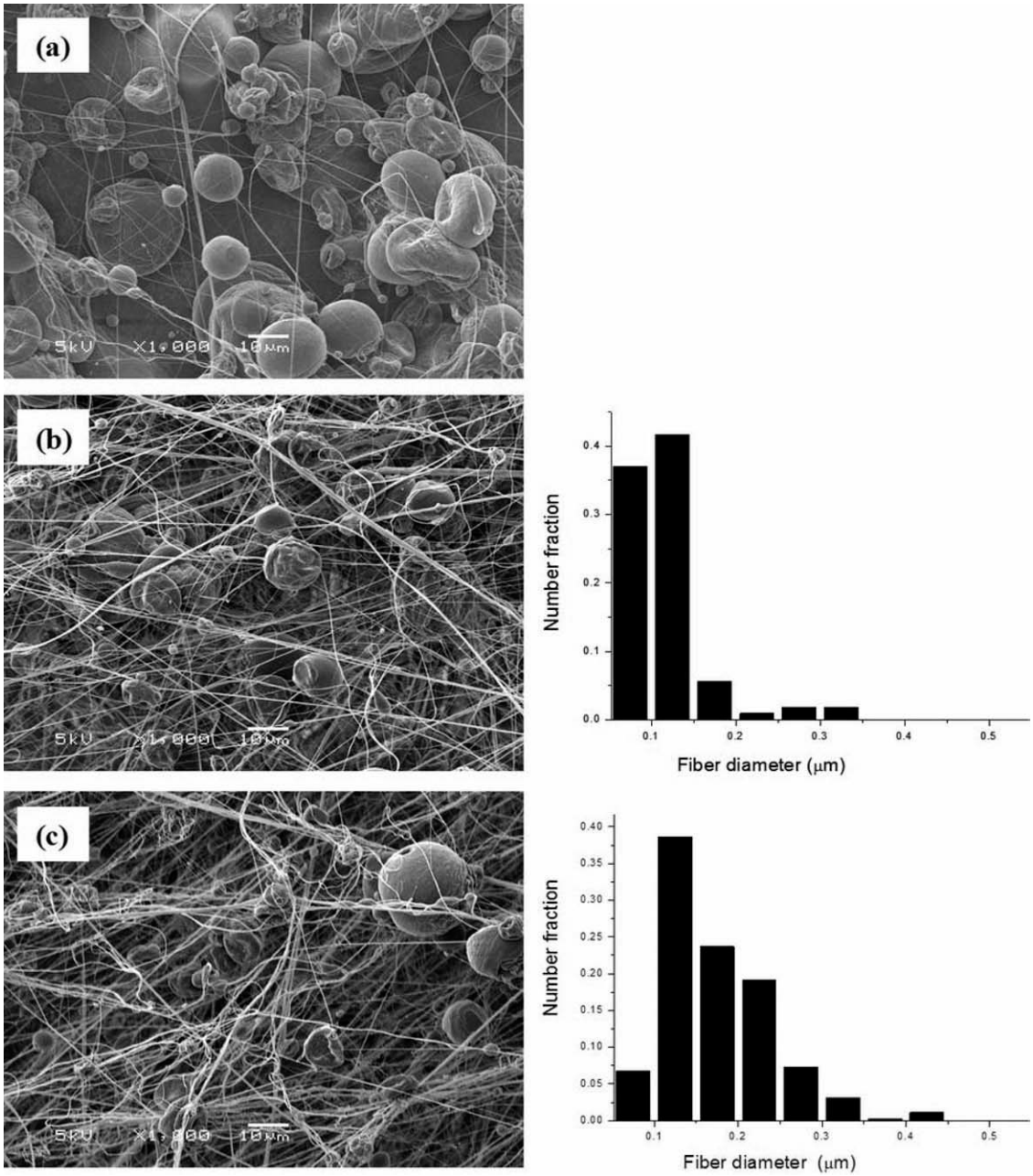

Figure 5 SEM images of fiber formations obtained using 12% PC solution at air pressures of (a) 0.1 MPa, (b) 0.3 MPa (with diameter distribution on the right), and (c) 0.5 MPa (with diameter distribution on the right).

the air blowing pressure was increased from 0.0 to 0.3 MPa, the average fiber diameter decreased from 0.168 to 0.120 μm for the 12% PC solution. The average fiber diameter of the nanofibers reached a minimum at an air blowing pressure of 0.3 MPa. When the air blowing pressure was at 0.5 MPa, the average fiber diameter increased to 0.169 μm, implying that the electrospinning process has optimal conditions. Similar results were found for other polymer concentrations. When the concentration of the PC solution was increased from 12 to 16%, the average fiber diameter of air blowing-assisted electrospun nanofibers increased from 0.120 to 0.166 μm at an air blowing pressure of 0.3 MPa. In the air blowing-assisted electrospinning process, air blowing enhances the stretching of the polymer solution jet and results in the stretching, bending, and movement of polymer fiber toward the grounded plate. This in turn increases the splitting of the polymer droplets, resulting in a decrease in the average diameter of air blowing-assisted electrospun nanofibers. In general, an increase of the air blowing pressure increases the air blowing rate. An increase of the air blowing rate at the outer nozzle accelerates the evaporation rate

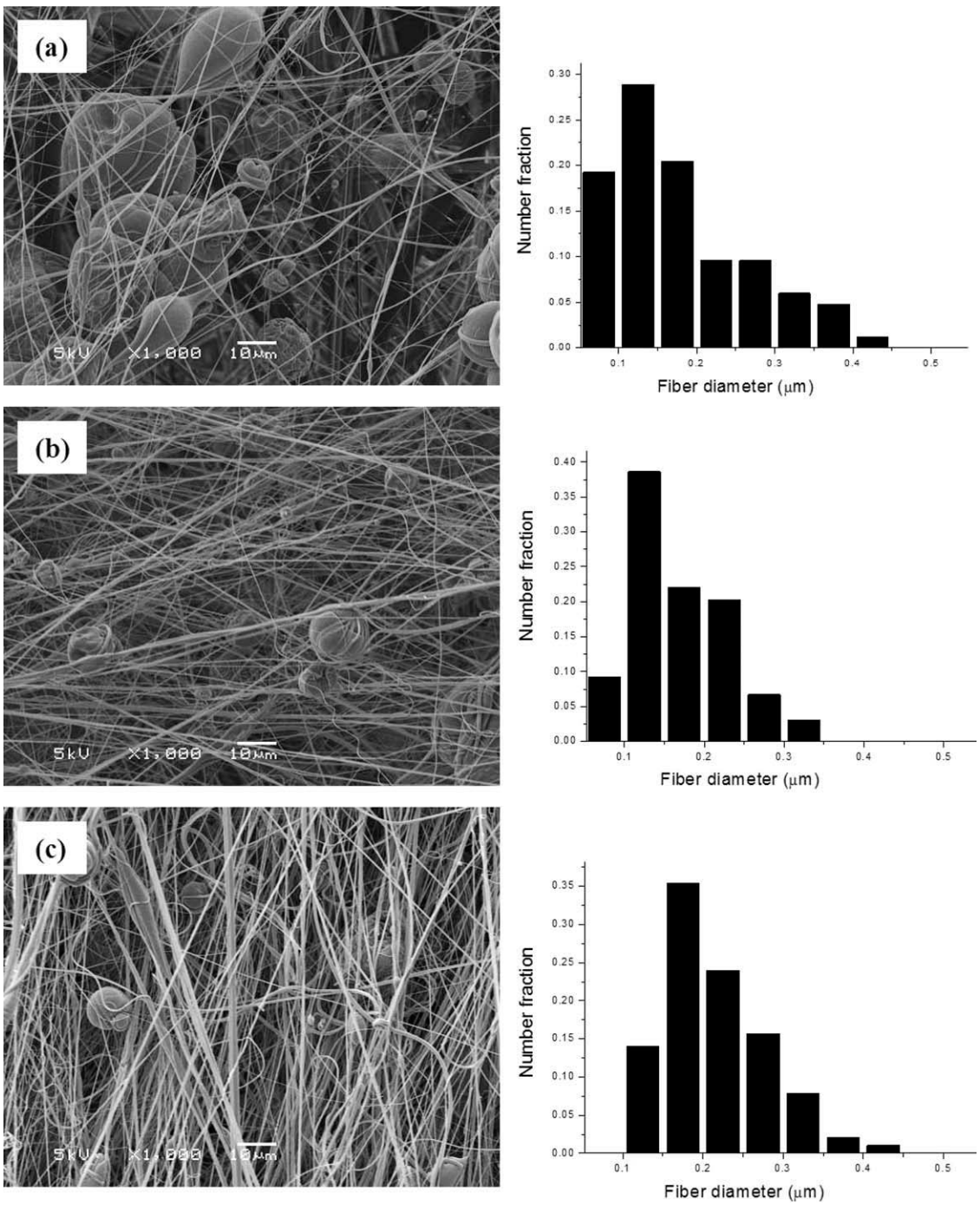

Figure 6 SEM images and diameter distributions of fiber formations obtained using 14% PC solution at air pressures of (a) 0.1 MPa, (b) 0.3 MPa, and (c) 0.5 MPa.

of solvents from the surface of the charged jet, which leads to earlier formation of fibers. For the 12% PC solution, electrospinning without air blowing resulted in the droplets and beads bonded to form film-like structures [Fig. 4(a)]. As the air blowing rate increased, the bonding stopped and more fibers with a few beads formed (Fig. 5). This indicates that an increase in the air blowing rate speed up the evaporation of solvents, which reduced the bonding of fibers and increased the driving force to produce thinner fibers with fewer beads. However, a further increase in the air blowing rate (air blowing pressure over 0.3 MPa) decreased the flight time and splitting time of the charged jet, which led to an increase in the average diameter of the PC electrospun nanofibers.[36] Therefore, the evaporation of the solvent and the stretching of PC chains induced by air blowing pressure significantly affect the average diameter

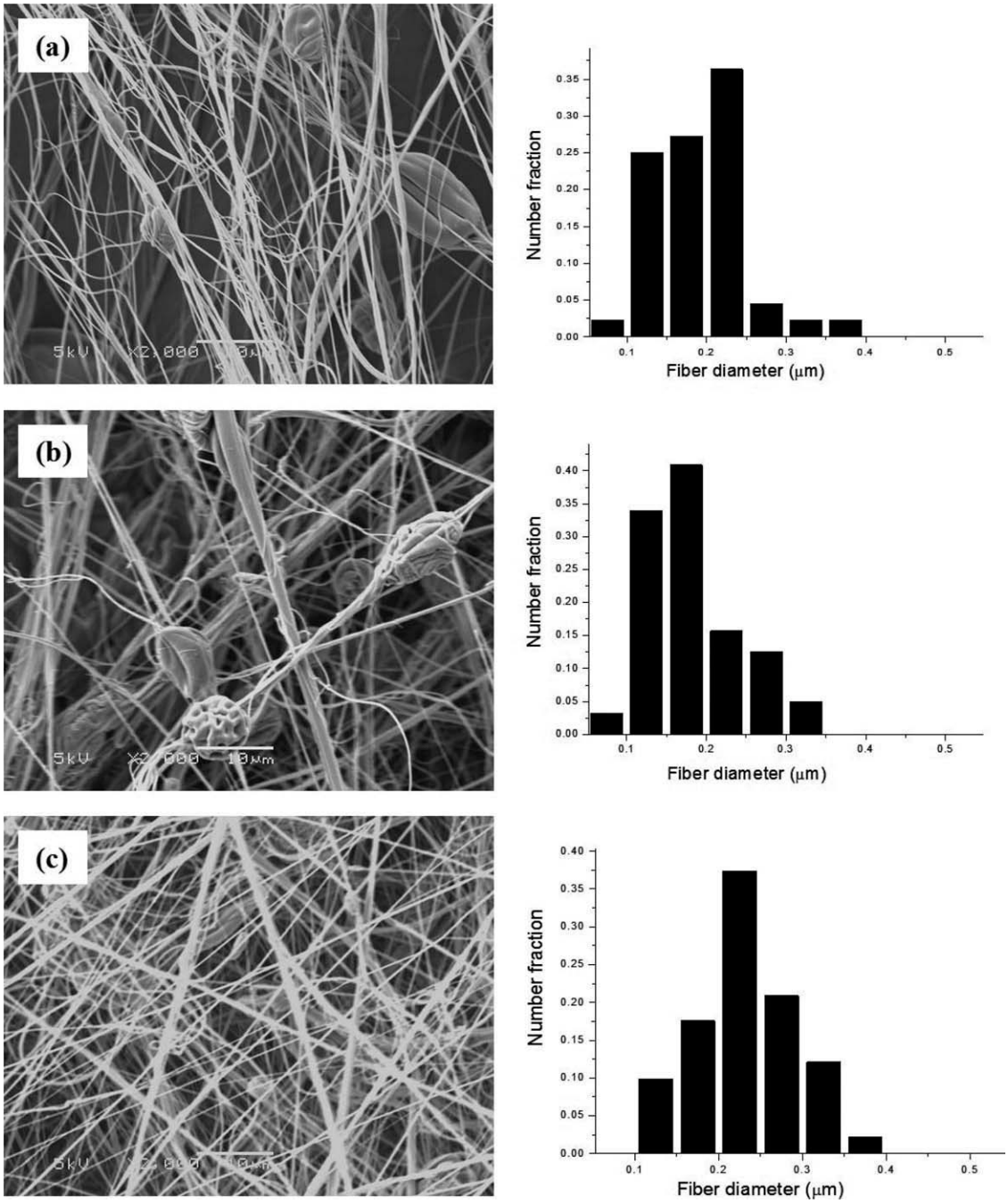

Figure 7 SEM images and diameter distributions of fiber formations obtained using 16% PC solution at air pressures of (a) 0.1 MPa, (b) 0.3 MPa, and (c) 0.5 MPa.

and morphology of the PC nanofibers during air blowing-assisted electrospinning.

Air permeability and mean flow pore size of PC nanofiber mat/PP nonwoven web

Since the nanofibers obtained from 16% PC solution had a lower bead density and more fiber deposition than those of 12 and 14% PC solutions, the 16% PC solution samples were chosen to further investigate the effects of fabrication parameters, namely air blowing pressure and fiber diameter, on the Frazier air permeability and mean flow pore size of the nanofiber mat/PP nonwoven web. The effects of air blowing pressure and fiber diameter on the Frazier air permeability of a blowing-assisted electrospun web obtained from a 16% PC solution are shown in Figure 10. As can be seen, without air blowing pressure applied, the PC nanofiber mat/PP nonwoven web had a broad fiber diameter distribution from 0.125 to 0.285 μm and a wide distribution of Frazier air permeability. When air blowing pressures of 0.1, 0.3, and

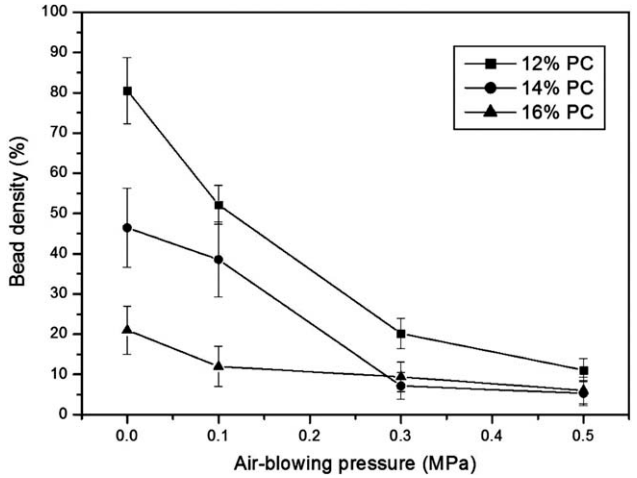

Figure 8 Effect of air blowing pressure on bead density for (a) 12%, (b) 14%, and (c) 16% PC solutions.

0.5 MPa were applied, the fiber diameters were in the ranges of 0.15∼ 0.22, 0.165∼ 0.23, and 0.22∼ 0.245 μm, respectively. An increase in the air blowing pressure narrows the distribution of the fiber diameter of the PC nanofiber mat/PP nonwoven web. At a 0.5-MPa air blowing pressure, a uniform fiber mat was obtained due to the narrow distribution of the fiber diameter, which led to a decrease of Frazier air permeability. Therefore, the fiber diameter distribution narrows and the Frazier air permeability decreases with increasing air blowing pressure. This indicates that the air blowing pressure has a negative effect on Frazier air permeability.

The effects of air blowing pressure and fiber diameter on the mean flow pore size of the PC nanofiber mat/PP nonwoven web were also investigated; the results are shown in Figure 11. Air blowing pressure and fiber diameter had similar effects on the mean flow pore size. Without air blowing, a high value of

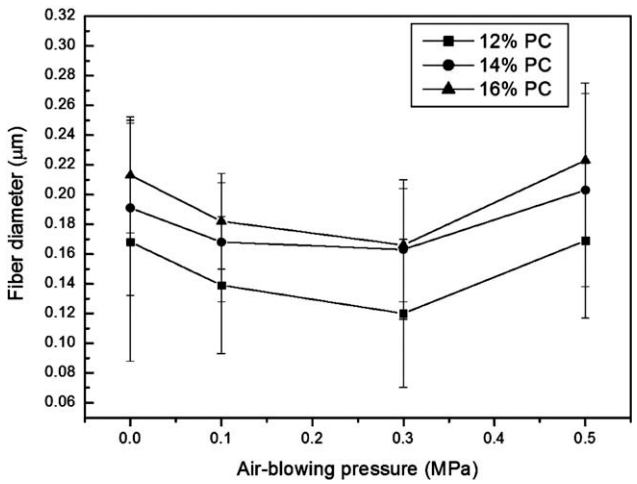

Figure 9 Effect of air blowing pressure on fiber diameter for (a) 12%, (b) 14%, and (c) 16% PC solutions.

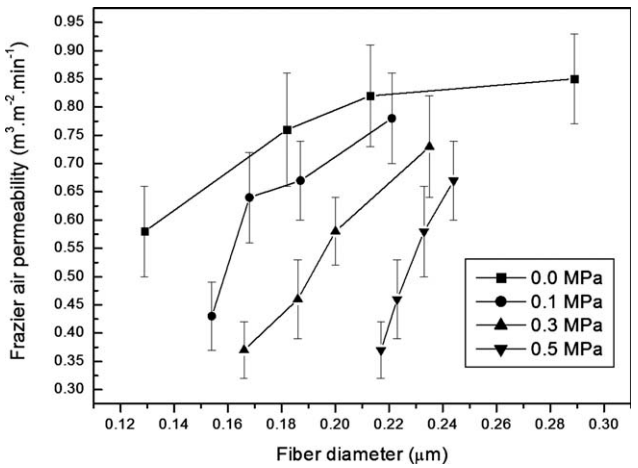

Figure 10 Effects of air blowing pressure and fiber diameter on Frazier air permeability of nanofiber mat/PP nonwoven web obtained using 16% PC solution. The applied voltage and the tip-to-collection-screen distance were 40 kV and 25 cm, respectively.

the mean flow pore size was obtained. When air blowing pressures of 0.1, 0.3, and 0.5 MPa were applied, the mean flow pore sizes of the electrospun nanofiber web varied in the ranges of 5.0∼ 8.0, 3.0∼ 6.7, and 2.2∼ 4.8 μm, respectively. Therefore, with the assistance of air blowing, the fiber diameter increased and the distribution of the fiber diameter narrowed, leading to a more uniform and denser PC nanofiber mat/PP nonwoven web, and consequently, a smaller mean flow pore size.

Filtration efficiency and pressure drop

Filtration efficiency and pressure drop are important parameters for filter media. Based on the results of

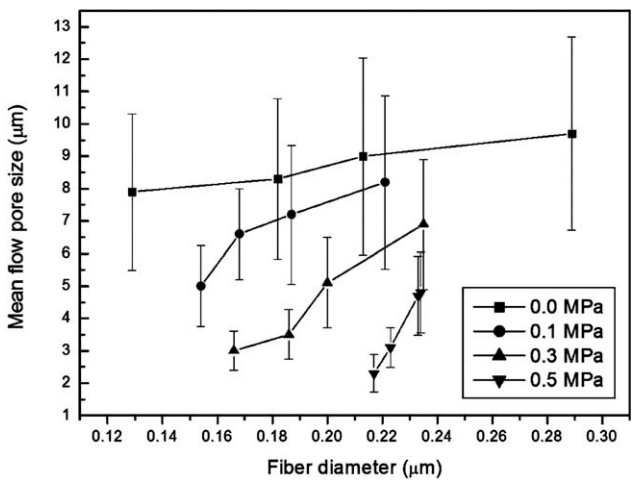

Figure 11 Effect of fiber diameter on mean flow pore size of nanofiber mat/PP nonwoven web obtained using 16% PC solution for various air blowing pressures. The applied voltage and the tip-to-collection-screen distance were 40 kV and 25 cm, respectively.

mean flow pore size of the electrospun web, the filtration performance of an air blowing-assisted electrospun nanofiber web fabricated using 16% PC solution was tested. The PC deposition amount of multiple-jet blowing-assisted electrospun nanofibers on the PP nonwoven sublayers was about 3.5–4.0 g/m^2. The average thickness of the PP nonwoven web was 74.0 μm. The mean flow pore sizes of nanofiber mat/PP nonwoven web were 3.1, 3.5, 6.6, and 8.3 μm, corresponding to average thicknesses of deposited electrospun layers of 50.6, 48.2, 42.6, and 42.2 μm, respectively. Figure 12 shows the filtration efficiencies under face velocities in the range of 2.67–13.33 cm/s and mean flow pore sizes in the range of 3.1–8.3 μm. As shown in Figure 12, the filtration efficiency of the PC nanofiber mat/PP nonwoven web decreased from 98 to 86% at a 2.67 cm/s surface velocity. With an increase in the surface velocity, more particles penetrated through the PC nanofiber mat/PP nonwoven web, resulting in an obvious reduction of filtration efficiency. The filtration efficiency was evaluated using an aerosol of 0.3-μm NaCl particles. A high face velocity led to strong penetration, resulting in the NaCl particles not being easily captured on the web surface and thus a reduced filtration efficiency.

The dependence of the pressure drop of a multiple-jet electrospun web on the mean flow pore size and face velocity is shown in Figure 13. It can be seen that the pressure drop decreased with increasing mean flow pore size of the PC nanofiber mat/PP nonwoven web. At a surface velocity of 2.67 cm/s, a small difference of pressure drop was observed. With increasing surface velocity, the reduction of pressure drop became larger, reaching a maximum of 5.0 mm H_2O at 13.33 cm/s, which translates into more resistance to air flow through the media. The high filtration efficiency and pressure drop can be attributed to the small mean flow pore size that resulted from the air blowing. The air blowing pressure induced a stretching force, which is similar to an electrical voltage, leading to an effective pulling force that forms uniform and high spin-draw ratio fibers with a narrow distribution of the fiber diameter and a small mean flow pore size of the electrospun mat/PP nonwoven web.

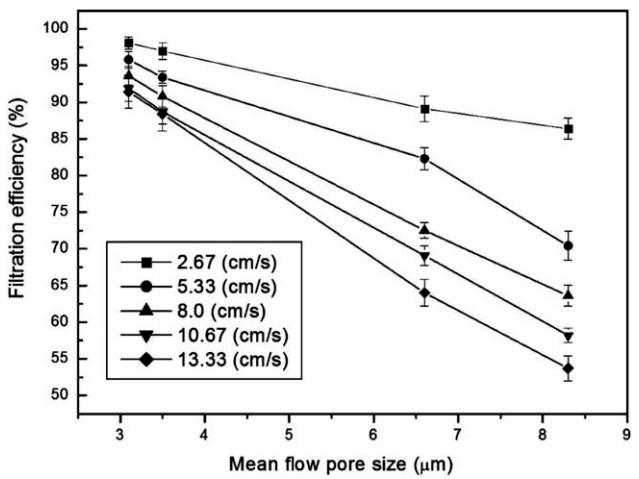

Figure 12 Effect of mean flow pore size on filtration efficiency of nanofiber mat/PP nonwoven web obtained from 16% PC solution for various face velocities. The applied voltage, polymer feeding flow rate, and the tip-to-collection-screen distance were 40 kV, 2.25 mL/h, and 25 cm, respectively.

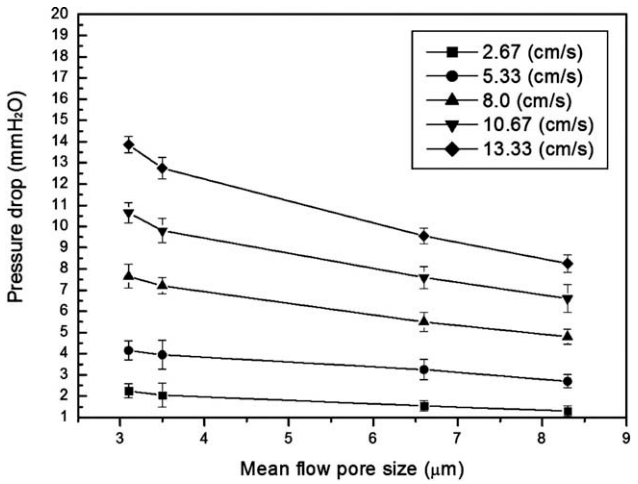

Figure 13 Effect of mean flow pore size on pressure drop of nanofiber mat/PP nonwoven web obtained from 16% PC solution for various face velocities. The applied voltage, polymer feeding flow rate, and the tip-to-collection-screen distance were 40 kV, 2.25 mL/h, and 25 cm, respectively.

CONCLUSION

PC nanofibers were fabricated via the air blowing-assisted electrospinning of PC solutions in a solvent of DMAc/THF. The effects of electrospinning process parameters, namely air blowing pressure and PC solution concentration, on the nanofiber morphology and the properties of the nanofiber mat were examined. SEM images, bead density calculations, and fiber diameter measurements indicate that an air blowing pressure of 0.3 MPa with a 16% PC solution are the optimum conditions for the fabrication of PC nanofibers. The air blowing pressure is the predominant factor in fiber formation. The filtration efficiency of the air blowing-assisted electrospun web was much higher than that of the nanofiber mat produced using conventional electrospinning. Air blowing enhances the stretching of the polymer solution jet and results in the stretching, bending, and movement of polymer fiber toward the grounded plate. The process investigated in this study produced PC nanofiber mats with few beads, a small mean flow pore size, and good filtration performance.

References

1. Huang, Z. M.; Zhang, Z. Y.; Kotaki, M.; Ramakrishna, S. Compos Sci Technol 2003, 63, 2223.
2. Hegde, R. R.; Dahiya, A.; Kamath, M. G. Available at: http://web.utk.edu/~mse/pages/Textiles/Nanofiber%20Nonwovens.htm. Accessed June 2010.
3. Moon, K. S.; Kim, H. J.; Lee, E.; Lee, M. Angew Chem Int Ed 2007, 46, 6807.
4. Feng, L.; Li, S.; Li, H.; Zhai, J.; Song, Y.; Jiang, L.; Zhu, D. Angew Chem Int Ed 2002, 41, 1221.
5. Reneker, D. H.; Chun, I. Nanotechnology 1996, 7, 216.
6. Formhals, A. U.S. Pat.1,975,504 (1934).
7. Lu, C.; Chen, P.; Li, J.; Zhang, Y. Polymer 2006, 47, 915.
8. Kim, S. J.; Nam, Y. S.; Rhee, D. M.; Park, H. S.; Park, W. H. Eur Polym J 2007, 43, 3146.
9. Marks, M. J.; Sekinger, J. K. Polymer 1995, 36, 209.
10. Yang, D.; Wang, Y.; Zhang, D.; Liu, Y.; Jiang, X. Chin Sci Bull 2009, 54, 2911.
11. Shawon, J.; Sung, C. J Mater Sci 2004, 39, 4605.
12. Krishnappa, R. V. N.; Desai, K.; Sung, C. J Mater Sci 2003, 38, 2357.
13. Moon, S.; Farris, R. J. Polym Eng Sci 2008, 48, 1848.
14. Welle, A.; Kröger, M.; Döring, M.; Niederer, K; Pindel, E.; Chronakis, I. S. Biomaterials 2007, 28, 2211.
15. Higgins, B. A.; Britain, W. J. Eur Polym J 2005, 41, 889.
16. Barhate, R. S.; Ramakrishna S. J Membr Sci 2007, 296, 1.
17. Qin, X. H.; Wang, S. Y. J Appl Polym Sci 2006, 102, 1285.
18. Dotti, F.; Varesano, A.; Montarsolo, A.; Aluigi, A.; Tonin, C.; Mazzuchetti, G. J Ind Text 2007, 37, 151.
19. Yarin, A. L.; Koombhongse, S.; Reneker, D. H. J Appl Phys 2001, 90, 4836.
20. Pana, H.; Li, L.; Hua, L.; Cuia, X. Polymer 2006, 47, 4901.
21. Feng, J. J. J Non-Newton Fluid Mech 2003, 116, 55.
22. Feng, J. J. Phys Fluids 2002, 14, 3912.
23. Hohman, M. M.; Shin, M.; Rutledge, G.; Brenner, M. P. Phys Fluids 2001, 13, 2201.
24. Reneker, D. H.; Yarin, A. L.; Fong, H.; Koombhongse, S. J Appl Phys 2000, 87, 4531.
25. Carroll, C. P.; Joo, Y. L. J Non-Newton Fluid Mech 2008, 153, 130.
26. Han, T.; Yarin, A. L.; Reneker, D. H. Polymer 2008, 49, 1651.
27. Yu, J. H.; Fridrikh, S. V.; Rutledge, G. C. Polymer 2006, 47, 4789.
28. Kong, C. S.; Yoo, W. S.; Lee, K. Y.; Kim, H. S. J Mater Sci 2009, 44, 1107.
29. Theron, S. A.; Yarin, A. L.; Zussman, E.; Kroll, E. Polymer 2005, 46, 2889.
30. Ding, B.; Kimura, E.; Sato, T.; Fujita, S.; Shiratori, S. Polymer 2004, 45, 1895.
31. Dosunmu, O. O.; Chase, G. G.; Kataphinan, W.; Reneker, D. H. Nanotechnology 2006, 17, 1123.
32. Wang, X.; Um, I. C.; Fang, D.; Okamoto, A.; Hsiao, B. S.; Chu, B. Polymer 2005, 46, 4853.
33. Um, I. C.; Fang, D.; Hsiao, B. S.; Okamoto, A.; Chu, B. Biomacromolecules 2004, 5, 1428.
34. Peng, M.; Sun, Q.; Ma, Q.; Li, P. Micropor Mesopor Mater 2008, 115, 562.
35. Lin, Y.; Yao, Y.; Yang, X. Wei, N.; Li, X.; Gong, P.; Li, R.; Wu, D. J Appl Polym Sci 2008, 107, 909.
36. Wang, B.; Yao, Y.; Peng, J.; Lin, Y.; Liu, W.; Luo, Y.; Xiang, R.; Li, R.; Wu, D. J Appl Polym Sci 2009, 114, 883.
37. Image, J. Available at: http://rsb.info.nih.gov/ij/. Accessed June 2010.
38. Kattamuri, N.; Sung, C. Nanotech 2004. Available at: http://www.nsti.org/publications/Nanotech/2004/pdf/B3-112.pdf. Accessed June 2010.
39. Megelski, S.; Stephens, J. S.; Chase, D. B.; Rabolt, J. F. Macromolecules 2002, 35, 8456.
40. Shenoy, S. L.; Bates, W. D.; Frisch, H. L.; Wnek, G. E. Polymer 2005, 46, 3372.
41. Fong, H.; Chun, I.; Reneker; D. H. Polymer 1999, 40, 4585.
42. Gupta, P.; Elkins, C.; Long, T. E.; Wilkes, G. L. Polymer 2005, 46, 4799.